

Special
Collection

Membrane Transport, Molecular Machines, and Maxwell's Demon

Stefan Borsley*^[a]

The spontaneous generation of transmembrane gradients is an important fundamental research goal for artificial nanotechnology. The active transport processes that give rise to such gradients directly mirror the famous Maxwell's Demon thought experiment, where a Demon partitions particles between two chambers to generate a nonequilibrium state. Despite these similarities, discussion of Maxwell's Demon is absent in the literature on artificial membrane transport. By contrast, the

emergence of rational design principles for nonequilibrium artificial molecular motors can trace its intellectual roots directly to this famous thought experiment. This perspective highlights the links between Maxwell's Demon and nonequilibrium machines, and argues that understanding the implications of this 19th century thought experiment is crucial to the future development of transmembrane active transport processes.

Introduction

The question of how to escape equilibrium has formed an important avenue of research across numerous disciplines for over a century.^[1] The question traces its intellectual roots to the thought experiments of James Clerk Maxwell^[2] and others^[3] (Figure 1A). These thought experiments depict the movement of particles between two compartments to result in the spontaneous generation of a nonequilibrium gradient. Application of information thermodynamics served to finally exorcise Maxwell's Demon,^[4] reconciling the seemingly paradoxical thought experiments with the Second Law of Thermodynamics through the treatment of information as a thermodynamic quantity.^[5]

Crucially, exploration and analysis of these pioneering thought experiments has directly led to formulation of rational design principles for nonequilibrium molecular machines, known as Brownian ratchet mechanisms.^[6] In this context, mechanically interlocked structures^[7] have been a vital tool for the translation of principles from physics into a chemical reality, due to the well-defined large-amplitude relative motion of their components.^[8] Interlocked structures effectively allow for the creation of artificial compartments in solution,^[6b] with macrocycle binding sites serving as the compartments and the macrocycle itself representing the particle to be transported (Figure 1B). The use of these mechanically interlocked architec-

tures as artificial proxies for the compartments of Maxwell's thought experiment has proved to be a highly fruitful approach for elucidating the principles of nonequilibrium transport.^[6] The underlying ratchet mechanisms that drive nonequilibrium processes have been extensively studied,^[9] and by employing simple interlocked machines, systematic variation of different parameters has enabled experimental verification of mathematical predictions.^[10]

Despite the increasing understanding of how to drive nonequilibrium processes in the context of molecular machines,^[6,8,9] concepts like Maxwell's Demon^[2] and ratcheting^[6d] remain virtually unexplored within the context of artificial membrane transport.^[11] Membranes (for example phospholipid bilayers) create physical compartments in a direct echo of Maxwell's Demon (Figure 1C). Biology employs the controlled generation (and dissipation) of transmembrane gradients as a convenient and rapidly accessible energy store in almost every example of sophisticated task performance.^[12] By contrast, developing artificial methods to control the movement of material across membranes remains a substantial challenge even where the movement is passive,^[11] i.e. thermodynamically downhill. Only a handful of examples of artificial active transport have been reported.^[13] This perspective discusses the concept of Maxwell's Demon^[2] and related thought experiments,^[3] highlighting their relevance to molecular machines.^[6b] This progress is contrasted with developments in the field of membrane transport.^[11,14] Finally, general approaches for how nonequilibrium membrane transport might be developed are discussed.

Maxwell's Demon

In 1867 James Clerk Maxwell proposed^[2] an imaginary being that could partition randomly moving particles between two chambers to generate a nonequilibrium state. Maxwell's Demon operates a frictionless gate (i.e. opening and closing the gate costs no energy) to allow high energy (fast moving, hot)

[a] Dr. S. Borsley
Department of Chemistry
Durham University
Lower Mountjoy, Stockton Road, Durham DH1 3LE, UK
E-mail: stefan.h.borsley@durham.ac.uk

Part of the Special Collection Systems Chemistry Talents. Stefan Borsley has been nominated for the special collection Systems Chemistry Talents by Board Member Scott Hartley.

© 2024 The Authors. ChemSystemsChem published by Wiley-VCH GmbH. This is an open access article under the terms of the Creative Commons Attribution License, which permits use, distribution and reproduction in any medium, provided the original work is properly cited.

particles to pass in one direction and low energy (slow moving, cold) particles to pass in the other. Controlling the average direction of particles in this way rectifies their movement based on their speed and thus creates a temperature gradient. Similarly, the system can be envisaged to create a pressure gradient (Figure 1A). In this case, the Demon opens the gate when a particle approaches from the left, allowing it to move from left to right, but shuts the gate when a particle approaches from the right, thus trapping it in the right chamber and forming a pressure gradient.

Since opening and closing the gate costs no energy, the Demon appears to create a nonequilibrium state at no apparent energetic cost, in direct contravention of the Second Law of Thermodynamics. The Second Law survives, however, as the Demon must use energy in the form of information to 'know' where to put each particle.^[4] Further related thought experiments – notably from Lippman,^[3a] Smoluchowski,^[3b,c] Szilárd,^[3d] and Feynmann^[3e] – have proposed related systems which discuss the generation of a gradient between compartments. Such thought experiments are directly related to physical systems which generate a nonequilibrium state.^[6d]

Compartmentalised Molecular Machines

Mechanically interlocked architectures have been crucial to the development of molecular machines,^[7] as they allow for well-defined large-amplitude co-conformational movement of the macrocycle relative to the track (an axle for rotaxanes or a second macrocycle for catenanes).^[8] These structures have allowed for the development of stimuli-responsive switches and shuttles.^[7,15] An important design feature that emerged was the consideration of the macrocycle as a particle to be transported and the track as a potential energy surface on which the particle can move (Figure 2).^[6] This view of mechanically interlocked molecules starts to directly echo the elements of the Maxwell's Demon thought experiment, with a particle (the macrocycle) being transported between compartments (binding sites on the track) (Figure 1B). Indeed, this view was crucial for progressing from simple switches^[15] to the development of nonequilibrium motors and pumps.^[6,16,17]

Through a series of papers in the 2000s Kay and Leigh translated^[6] the concept of ratcheting from the physics



Stefan Borsley obtained his MChem from the University of Manchester (2011) and PhD from the University of St Andrews (2015) under the supervision of Dr. Euan Kay. He subsequently undertook postdoctoral research at the University of Edinburgh with Prof. Scott Cockroft and the University of Manchester with Prof. David Leigh. He now holds a Royal Society University Research Fellowship at Durham University, where his research focusses on understanding and controlling dynamic nonequilibrium processes in compartmentalised systems.

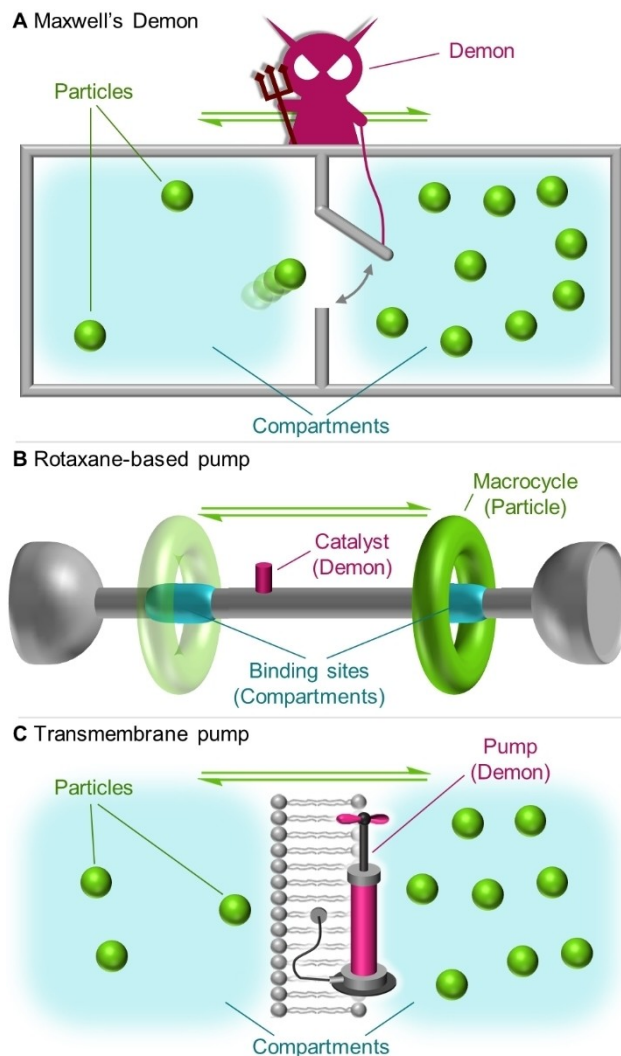


Figure 1. Nonequilibrium transport processes. (A) A Maxwell's pressure Demon. The Demon opens and closes a frictionless gate in response to the approach of a particle.^[2] This process rectifies the random movement of the particles, allowing them to move only from the left compartment to the right compartment, creating a pressure gradient. (B) A rotaxane-based molecular pump.^[10] The random motion of the macrocycle shuttling is rectified to pump the macrocycle distribution to the right-hand binding site. Catalysis of a fuel-to-waste reaction proceeds at different rates depending on the location of the macrocycle, driving the nonequilibrium transport through an information ratchet mechanism. (C) A transmembrane pump. The motion of the particles (ions or molecules) can be rectified through use of a pump, which harnesses an energy source to drive nonequilibrium transmembrane transport.

literature to a chemical reality. Molecular ratchet mechanisms were described allowing for the identification of the minimal elements of both energy ratchets – where kinetic control dictates the statistically determined direction of relaxation following the fluctuation of bulk conditions that change the equilibrium position of the particle – and information ratchets – where differences in reaction rates between (co-)conformations kinetically bias the direction of movement.^[6d] In 2006,^[6b] macrocycle binding sites on rotaxane and catenane-based molecular machines were explicitly equated with the compartments of Maxwell's Demon. In 2007^[6c] this research culminated in a

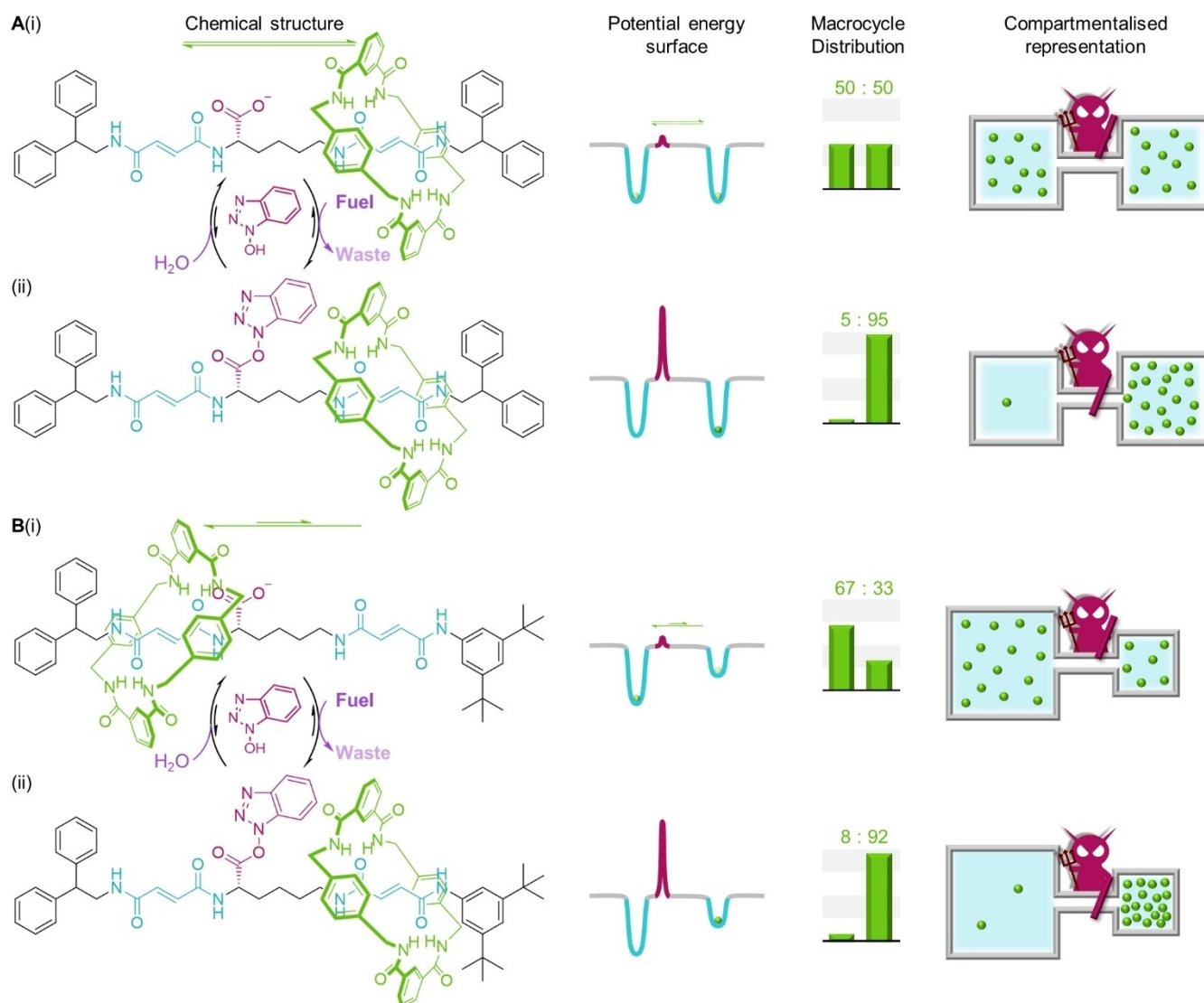


Figure 2. Mechanically interlocked molecules as compartmentalised molecular machines. (A) A rotaxane-based chemically fuelled autonomous molecular pump.^[10a] (i) At equilibrium, the macrocycle distribution is 50:50 as the two macrocycle binding sites have equal energy. This can be represented as a two-compartment machine with an equal distribution of particles. (ii) Upon fuelling the rotaxane with a carbodiimide in the presence of hydroxybenzotriazole (HOBt), the carboxylate catalyst on the machine catalyses the hydration of the carbodiimide, forming an OBt ester, which is hydrolysed to complete the catalytic cycle. Differences in the rate of ester formation and hydrolysis depending on the macrocycle generate kinetic asymmetry, resulting in pumping of an entropically disfavoured nonequilibrium steady state. As the energy of the binding sites is unaffected, the compartmentalised representation (right) directly resembles Maxwell's demon. (B)(i) Varying well-depths of one of the macrocycle binding sites effectively changes the size of the compartments.^[10c] (ii) Upon fuelling, the pump now kinetically drives the macrocycle to an enthalpically as well as entropically unfavoured site.

rotaxane-based information ratchet that used light to measure the position of the macrocycle and open/close a gate to create a direct molecular analogue of Maxwell's Demon, able to spontaneously generate a gradient.

More recently, Leigh has developed a series of autonomous chemically fuelled machines,^[10,17] where the energy that drives nonequilibrium behaviour is supplied through an exergonic fuel-to-waste reaction.^[18] These chemically fuelled artificial motors and pumps^[10,17] operate through an information ratchet mechanism,^[8] where the reaction rates for the machine-catalysed fuel-to-waste conversion depend on the macrocycle position, and thus serve to 'measure' the position of the system and drive it out of equilibrium.

At equilibrium, the macrocycle of a rotaxane-based molecular ratchet^[10a] (Figure 2A(i), left) is evenly distributed between both compartments across the population of rotaxanes, and is free to shuttle between the two binding sites. This can be represented as a potential energy surface, showing two equal wells or as a pair of linked compartments with evenly distributed particles (Figure 2A(i), right). The rotaxane catalyses a carbodiimide-to-urea^[9] fuel-to-waste reaction.^[18] Differences in the rate of reaction of (i) the rotaxane with the fuel and (ii) the hydrolysis of the transient oxybenzotriazole barrier dependent on the macrocycle position constitute the kinetic asymmetry^[9] of the system, and result in pumping of the macrocycle distribution towards the right-hand (distal) binding

site (Figure 2A(ii)). Crucially, the binding sites are unchanged, so the well-depths remain constant. By looking at the compartmentalised scheme representation (Figure 2, right), it can be considered that a nonequilibrium state analogous to Maxwell's Demon has been achieved (Figure 2A(ii), right). Systematic structural variations enable exploration of this system.^[10b-d] For example, varying the binding strength of one of the compartments allows pumping between unevenly sized compartments^[10c] (Figure 2B). Alternatively, changing the structure of the fuel allows the kinetic asymmetry to be varied^[10b] – effectively changing how well the Demon is able to measure the position of the system.

The information ratchet mechanisms that drive the non-equilibrium behaviours of such mechanically interlocked machines have been shown to drive virtually all known biological machines,^[9,12,20] including transmembrane pumps such as ATP synthase.^[20] It seems reasonable, therefore, to consider the application of such mechanisms in the context of artificial membrane transport.

Artificial Channels and Ionophores

Artificial transmembrane transport is a well-developed field.^[11,14] The focus has generally been on developing means to transport charged, hydrophilic ions across a hydrophobic lipid bilayer membrane. Broadly speaking, transporters fall into two categories, channels and carriers.^[11] Channels are essentially membrane-spanning tubes, through which ions can flow (Figure 3A). Carriers are lipid soluble molecules that can freely diffuse between the two faces of the membrane (Figure 3B). Carriers can bind an ion, screening the charge and thus allowing diffusion across the hydrophobic membrane. Orthogonal stimuli can modulate the ion transport activity of both channels^[21] (Figure 3C) and carriers^[22] (Figure 3D). While channels can simply be blocked,^[21a-d] more sophisticated approaches such as photoswitching to regulate channel size^[21e-h] or addition/removal of ligands/metals to induce channel assembly/disassembly^[21i-l] have also been developed. Building on the complexity of stimuli-responsive channel formation, Fyles has reported the transient formation of ion channels in response to a chemical input.^[23] Transient thioester formation activates the channel forming compound, allowing temporal control over ion channel formation. Photoswitching has also been demonstrated as a convenient way of inducing conformational change to regulate carrier activity.^[22]

When considering ion transport from a molecular machines perspective, the diffusion of a carrier between the two faces of a membrane can be viewed as paralleling the shuttling of a macrocycle between two binding sites. In recent years a number of 'anchored carriers',^[14d] where the carrier can diffuse across the membrane but is tethered to a static 'anchor', have also been developed. While such developments highlight the link between molecular machines and transmembrane shuttling,^[14d] simple, unanchored carriers alone already display this shuttling behaviour when considering the membrane as part of the system. The switching of carrier binding affinity^[22]

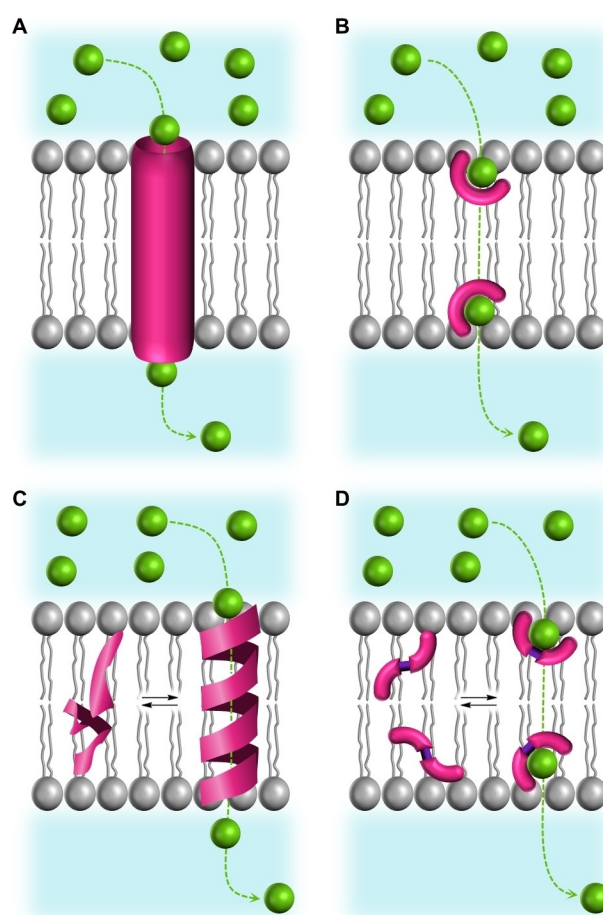


Figure 3. Schematic representations of artificial transporters employed for passive transmembrane ion transport.^[11] (A) Transmembrane channels allow the passage of ions across a membrane. (B) Carriers bind ions, screening the charge and allowing the carrier-ion complex to diffuse across the membrane. (C) Switchable channels^[21] and (D) switchable carriers^[22] allow for orthogonal control over ion transport.

might be seen to reflect the switching of a rotaxane-based molecular machine to either allow or prevent macrocycle shuttling. However, when considering the development of a transmembrane pump, the switching of states is only conducted at the microscopic level in response to positional information of an individual particle, rather than on the ensemble level in response to a change in conditions. In other words, while switching might occur at an individual particle level, the ensemble system maintains a constant steady state. Consequently, a different approach is required.

Artificial Transmembrane Pumps

Examples of artificial systems that perform active transport are extremely limited.^[13] As with small-molecule machines that pump macrocycles,^[10,16g,i,17b] artificial transmembrane ion pumps require a source of energy, and have generally employed light.

Shinkai's seminal work on azobenzene photoswitches included the use of azobenzene-based crown ethers for photo-

switchable control over sodium transport across a liquid membrane.^[22a-c] While the formation of gradients (i.e. active transport) was not demonstrated, subsequent simulation indicated that by employing orthogonal illumination of different wavelengths on either side of the membrane to control the rates of isomerisation in a spatially-defined manner, active transport would be possible.^[24] In 2014,^[13d] Bakker reported the light-driven pumping of protons across a liquid membrane (Figure 4). Irradiating a spiropyran/merocyanine photoacid dissolved in the membrane-phase with ultraviolet light induces a ring-opening reaction, converting spiropyran to merocyanine, whereas irradiation with visible light induces the reverse reaction. By selectively shining ultraviolet light on one side of the membrane and visible light on the other, the state of the photoacid could be spatially controlled. A proton is taken up by merocyanine, carried through the liquid membrane by random diffusion and released on the other side upon conversion of the merocyanine back to spiropyran. It is the modulation of the relative rates of switching as determined by the different wavelengths at either side of the membrane that generates kinetic asymmetry in the cycle, and thus allows pumping to be achieved.^[24] The photoacid can be considered as a Demon that

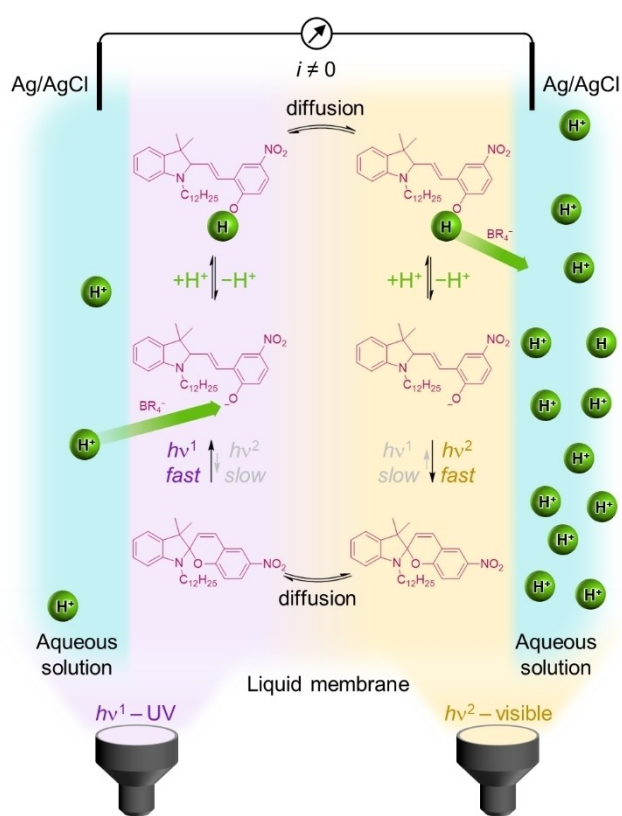


Figure 4. A photoacid-derived transmembrane proton pump developed by Bakker.^[13d] Opposite sides of a liquid membrane are irradiated at different wavelengths, inducing spatially defined photoswitching of a spiropyran photoacid. UV light on the left side of the membrane accelerates switching of the spiropyran to merocyanine. A proton is taken up from the aqueous phase and carried through the hydrophobic membrane by a lipophilic tetrakis[3,5-bis-(trifluoromethyl)phenyl] borate anion. The protonated merocyanine can diffuse across the membrane, where it is photoswitched by visible light back to the spiropyran, releasing the proton to the aqueous solution on the right.

measures the wavelength of the light to 'know' whether to pick up or release a proton, while randomly diffusing between the two interfaces.

Bakker's system^[13d] demonstrates that anisotropy (required to provide information to the Demon) can be generated by spatially differentiating the two sides of the membrane. This is difficult to achieve with light for phospholipid-bilayers due to their narrow width and high transparency to light. An alternative way of generating anisotropy in a transmembrane context is to directionally orientate molecules within a membrane,^[25] thus allowing the conditions and reagents in the aqueous compartments on either side to be the same.

In 1997,^[13a] Gust and Moore reported an autonomous light-driven transmembrane pump (Figure 5). The photoresponsive naphthoquinone-porphyrin-carotenoid (Q-P-C) molecule inserts with directional preference into the membrane. Upon irradiation, a diradical zwitterion pair is formed across the membrane, with a radical anion located on the naphthoquinone and a radical cation located on the carotenoid. Recombination of the radicals proceeds fastest when mediated by a freely dissolved 2,5-diphenylbenzoquinone carrier (Q₂), which can shuttle between the two sides of the membrane. The radical recombination is accompanied by the transport of a proton across the membrane. The difference in conditions at the interior and exterior of the membrane, dictated by the anisotropic membrane-insertion of the Q-P-C molecule, kinetically differentiates the pick-up and release of a proton, generating kinetic asymmetry in the cycle and allowing the pump to function. The light-driven transmembrane proton pump was able to transport sufficient protons to allow for the synthesis of ATP when operated in combination with ATP-synthase.^[13b] Furthermore, the structure of the carrier could be changed so carrier-mediated radical recombination was associated with pumping of Ca²⁺ instead of H⁺.^[13c]

Ratchets and Demons: Chemically Fuelled Membrane Transport

While light provides one means of supplying energy to drive transmembrane pumps, biology generally employs chemical fuels as a convenient, readily available, and readily transportable source of energy.^[18] Hydrolysis of adenosine triphosphate (ATP) provides energy for numerous biological machines,^[12,20] including pumps. ATP-Binding Cassette (ABC) transporters^[26] are a broad class of transmembrane proteins found in most cells across all lifeforms that facilitate the active transport of material into cells across the lipid bilayer membrane (Figure 6A). The mechanism of their action has been extensively described in the context of Maxwell's Demon.^[27] While missing some kinetic and biochemical detail of conformational changes, a coarse-grained four-state model provides a description of the nonequilibrium pumping achieved by the ABC transporters (Figure 6A(ii)). The transporters (pink) catalyse the hydrolysis of ATP fuel (dark purple) to form adenosine diphosphate (ADP) + inorganic phosphate (Pⁱ) waste (light

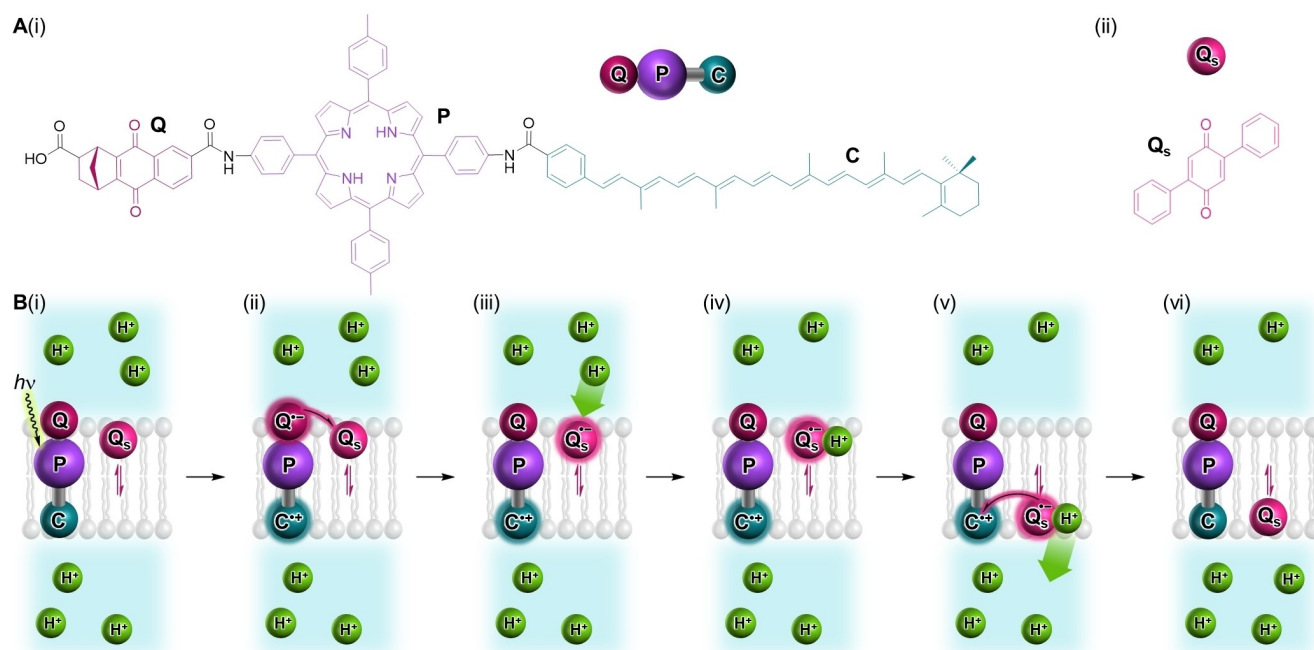


Figure 5. (A) Gust and Moore's pump,^[13a] composed of (i) a naphthoquinone-porphyrin-carotenoid (Q–P–C) molecule and (ii) a membrane-soluble 2,5-diphenylbenzoquinone carrier (Q_s). (B) Q–P–C is added to the exterior of a vesicle. Due to the carboxylate at one end of the molecule, it inserts into a membrane with the naphthoquinone moiety (Q) preferentially orientated towards the exterior of a vesicle. (i) Photoexcitation of the Q–P–C molecule leads to formation of (ii) the excited state diradical $Q^{\bullet-}$ –P–C $^{\bullet+}$. (iii) The radical is then transferred to membrane-soluble carrier 2,5-diphenylbenzoquinone Q_s to form Q–P–C $^{\bullet+}$ and $Q_s^{\bullet-}$. The $Q_s^{\bullet-}$ radical carrier rapidly picks up a proton from the exterior of the vesicle where it is formed to generate (iv) $Q_s^{\bullet}H$, which diffuses through the membrane, carrying the proton with it. (v) At the interior side of the membrane, $Q_s^{\bullet}H$ is oxidised by the Q–P–C $^{\bullet+}$ radical to regenerate the photocatalyst Q–P–C and form $Q_s^{\bullet+}H$ (step 5), which rapidly deprotonates to deliver the proton to the interior of the vesicle and (vi) regenerate Q_s . Q_s can subsequently diffuse back across the membrane to complete the cycle.

purple), and extract the energy to drive directional active transport of a substrate (green).^[18,27] Exchange of the $ADP + P^i$ waste for ATP fuel is associated with a conformational change that exposes a binding site for the substrate to the exterior of the membrane, while ATP hydrolysis causes the opposite conformational change, exposing the substrate binding site to interior of the membrane. Binding of the substrate allosterically modulates the $ADP \rightarrow ATP$ exchange reaction and the $ATP \rightarrow ADP$ hydrolysis reaction, thus generating kinetic asymmetry.^[9] The differences in reaction rates effectively allow the protein to measure the presence/absence of the substrate, and open/close the gate accordingly.

The mechanism of the ABC transporter (Figure 6A) maps directly to the mechanism of the small-molecule rotaxane based pumps described previously^[10] (Figure 6B, c.f. Figure 2). Here, reaction rates for ester formation and hydrolysis are dependent on the location of the macrocycle, driving kinetic formation of a nonequilibrium state through an information ratchet mechanism.^[6d,9] The information ratchet mechanism that drives ABC transporters^[27] and related autonomous mechanically-interlocked machines^[17a] has been extensively described through both trajectory thermodynamics^[9b,c] and information thermodynamics^[9d] approaches. Likewise, the understanding of the underlying mechanism that drives the nonequilibrium behaviour has enabled translation of the principles to a structurally distinct rotary motor^[17c] (Figure 6C). Here, the motor experiences different angular compartments, while the use of

chiral reagents serves to 'measure' the position of the system through differences in the enantioselective rates of anhydride formation/hydrolysis.

The mechanistic similarities between the ABC transporters^[27] (Figure 6A), a rotaxane-based pump^[10a] (Figure 6B) and a rotary motor^[17c] (Figure 6C) are striking. The information ratchet mechanism that drives them can be described in the language of Maxwell's Demon. The particle (substrate, macrocycle or rotor) can sample two compartments (sides of the membrane, macrocycle binding sites or rotational angular conformations for the ABC transporter, a rotaxane-based pump and a rotary motor, respectively). In each case, the rates of the reactions depending on the position of the particle determine the kinetic asymmetry and drive nonequilibrium motion. The well-developed understanding of nonequilibrium molecular machines^[9] and the identification of comparable mechanisms for biological transport^[27] augers well for the future rational design of membrane transport pumps, which can build on the understanding of small-molecule machines and apply the lessons in a transmembrane context.

Summary and Outlook

An impressive array of molecular machines has been developed.^[10,16,17] Among these are examples that can autonomously drive nonequilibrium motion or nonequilibrium states

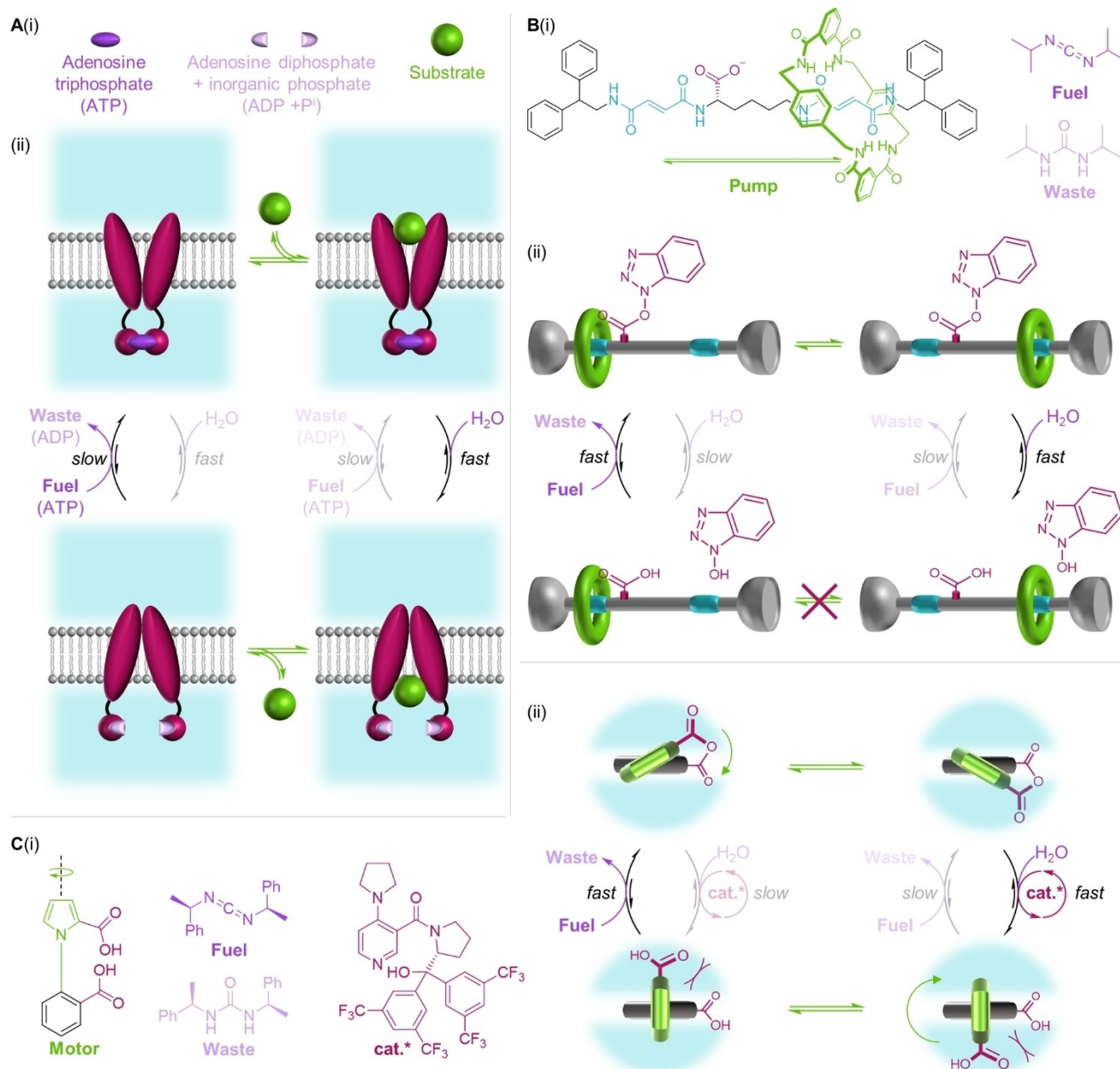


Figure 6. Biological transmembrane Maxwell's Demons and artificial molecular information ratchets. **(A)(i)** Schematic representations of the adenosine triphosphate (ATP) fuel, adenosine diphosphate (ADP) + inorganic phosphate (Pⁱ) waste and the substrate that is actively transported by ATP-Binding Cassette (ABC) transporters.^[26,27] **(ii)** The ABC transporter catalyses the fuel-to-waste reaction, involving a large-scale transmembrane conformational change of the protein structure within the catalytic cycle that transports the substrate across the membrane. The chemomechanical cycle shows that differences in the rates of ADP→ATP exchange (up arrows) and ATP hydrolysis (down arrows) depend on the allosteric binding of the substrate to the protein (horizontal equilibria), thus kinetically driving the substrate across the membrane. **(B)(i)** A chemically fuelled autonomous rotaxane pump and structures of the fuel and waste.^[10] **(ii)** The rotaxane catalyses the fuel-to-waste reaction, involving the formation of an oxybenzotriazole ester within the catalytic cycle that restricts movement of the macrocycle. The chemomechanical cycle shows that differences in the rates of ester formation (up arrows) and ester hydrolysis (down arrows) depend on the mechanical state (horizontal equilibria) of the rotaxane, thus kinetically driving the macrocycle (green) between the two binding site compartments (blue). **(C)(i)** A chemically fuelled autonomous rotary motor and structures of the fuel, waste and chiral catalyst.^[17c] **(ii)** Top-down schematic representation of the motor. The motor catalyses the fuel-to-waste reaction, involving the formation of a tethered anhydride between the two rings, allowing their relative rotation during the catalytic cycle. The chemomechanical cycle shows that differences in the rates of anhydride formation (up arrows) and anhydride hydrolysis (down arrows) depend on the mechanical state (horizontal equilibria) of the motor, thus kinetically driving the rotor (green) between the two angular compartments (blue).

in response to an energy input.^[10,16a,b,17] Crucial to the development of these machines has been the development of mechanically interlocked molecules,^[7] which allow for controlled large-amplitude motion between well-defined binding

sites.^[8] This has allowed for the translation of principles from physics,^[6] grounded in the Maxwell's Demon thought experiment, to develop an understanding of molecular ratchets.^[6d] These rules and mechanisms have now been applied beyond

mechanically interlocked molecules to drive rotation around a bond in a rotary motor,^[16c] and are also increasingly being recognised as a general means of driving nonequilibrium processes in other fields.^[9a,28]

Complementing the progress in the field of molecular machines, artificial membrane transport mechanisms based on channels and carriers have been developed.^[11,14,21–23] Limited examples of systems capable of active transport have been reported,^[13] most notably Gust and Moore's light-driven transmembrane pump.^[13a–c] However, these developments have been largely rooted in the development of photovoltaics and artificial photosynthesis,^[29] rather than molecular machines.

The field of artificial membrane transport is well-placed to leverage the principles of Maxwell's Demon that have been so instrumental in the development of nonequilibrium small molecule machines.^[6,10,16,17] The essential elements for driving nonequilibrium processes (e.g. anisotropy, an energy source, allosteric modulation of rates, kinetic asymmetry) are increasingly well-understood,^[9] and biology provides proof-of-concept transmembrane pumps^[12,20,26] that operate by the same information ratchet mechanisms.^[20,27] Crucial for to the development of transmembrane pumps will be learning how to control the kinetics of processes within complex reaction networks at the interface of lipid bilayers.^[19,30,31] Fyles's work on the transient formation of ion channels^[23] provides an important example of how kinetic control can be imparted on membrane-based systems. Future work might seek to develop general approaches to controlling the kinetics of substrate binding and release on opposite sides of a membrane, thus enabling active transport to be achieved and applied to a wide range of ions/molecules. Given biology's extensive use of forming and dissipating transmembrane gradients in almost every example of task performance,^[12,20] learning how to pump nonequilibrium gradients represents an important step towards developing our own artificial nanotechnologies.

Acknowledgements

S.B. is a Royal Society University Research Fellow.

Conflict of Interests

The authors declare no conflict of interest.

Keywords: nonequilibrium processes · membranes · rotaxanes · energy transfer · supramolecular chemistry

- [1] a) S. Carnot in *Reflexions sur la Puissance Motrice du Feu et sur les Machines Prepres a Developper cette Puissance* Bachelier, Paris, 1824; English translation H. Thurston, *Reflections on the Motive Power of Heat*, J. Wiley & Sons, New York 1890; b) N. Bohr, *Physical Science and the Problem of Life*, in *Atomic Physics and Human Knowledge*, Wiley, New York, 1958; c) E. Schrödinger, *What is life? The physical aspect of the living cell*. Cambridge University Press, Cambridge, UK, 1951; d) I. Prigogine, *Science* 1978, 201, 777–785; e) A. Pross, *What is Life?: How Chemistry Becomes Biology*, Oxford University Press, Oxford, UK 2016.

- [2] a) *Maxwell's Demon 2. Entropy, Classical and Quantum Information, Computing* (Eds.: H. S. Leff, A. F. Rex), Institute of Physics Publishing, Bristol, 2003. The first b) private and c) public written discussions of the 'temperature demon' were; b) J. C. Maxwell, *Letter to P. G. Tait*, 11 December 1867. Quoted by C. G. Knott in *Life and Scientific Work of Peter Guthrie Tait*, Cambridge University Press, London, 1911, pp 213–214; c) J. C. Maxwell in *Theory of Heat*, Longmans, Green and Co., London, 1871, Chapter 12.
- [3] a) G. Lippmann, *Rapp. Congr. Int Phys. Paris* 1900, 1, 546–550; b) M. von Smoluchowski, *Physik. Z.* 1912, 13, 1069–1080; c) M. von Smoluchowski, *Vorträge über die Kinetische Theorie der Materie und der Elektrizität* (Ed.: M. Planck), Teubner and Leipzig, Berlin, 1914, pp 89–121; d) L. Szilard, *Zeitschrift für Phys.* 1929, 53, 840–856; *Behav. Sci.* 1964, 9, 301–310; e) R. P. Feynman, R. B. Leighton, M. L. Sands in *The Feynman Lectures on Physics, Vol. 1*, Addison-Wesley Publishing Company, Reading, Massachusetts, 1963, Chapter 46.
- [4] T. Sagawa, M. Ueda, *Phys. Rev. Lett.* 2008, 100, 080403.
- [5] a) C. E. Shannon, *Bell Syst. Tech. J.* 1948, 27, 379–423; b) J. M. R. Parrondo, J. M. Horowitz, T. Sagawa, *Nat. Phys.* 2015, 11, 131–139.
- [6] a) J. V. Hernández, E. R. Kay, D. A. Leigh, *Science* 2004, 306, 1532–1537; b) M. N. Chatterjee, E. R. Kay, D. A. Leigh, *J. Am. Chem. Soc.* 2006, 128, 4058–4073; c) V. Serrelli, C.-F. Lee, E. R. Kay, D. A. Leigh, *Nature* 2007, 445, 523–527; d) E. R. Kay, D. A. Leigh, F. Zerbetto, *Angew. Chem. Int. Ed.* 2007, 46, 72–191.
- [7] a) J.-P. Sauvage, *Angew. Chem. Int. Ed.* 2017, 56, 11080–11093; b) J. F. Stoddart, *Angew. Chem. Int. Ed.* 2017, 56, 11094–11125.
- [8] E. R. Kay, D. A. Leigh, *Angew. Chem. Int. Ed.* 2015, 54, 10080–10088.
- [9] a) G. Ragazzon, L. J. Prins, *Nat. Nanotechnol.* 2018, 13, 882–889; b) R. D. Astumian, *Acc. Chem. Res.* 2018, 51, 2653–2661; c) R. D. Astumian, *Nat. Commun.* 2019, 10, 3837; d) S. Amamo, M. Esposito, E. Kreidt, D. A. Leigh, E. Penocchio, B. M. W. Roberts, *Nat. Chem.* 2022, 14, 530–537; e) S. Amamo, M. Esposito, E. Kreidt, D. A. Leigh, E. Penocchio, B. M. W. Roberts, *J. Am. Chem. Soc.* 2022, 144, 20153–20164; f) I. Arahamian, S. M. Goldup, *J. Am. Chem. Soc.* 2023, 145, 14169–14183; g) E. Penocchio, G. Ragazzon, *Small* 2023, 19, 2206188.
- [10] a) S. Borsley, D. A. Leigh, B. M. W. Roberts, *J. Am. Chem. Soc.* 2021, 143, 4414–4420; b) S. Borsley, D. A. Leigh, B. M. W. Roberts, I. J. Vitorica-Yrezabal, *J. Am. Chem. Soc.* 2022, 144, 17241–17248; c) L. Binks, S. Borsley, D. A. Leigh, E. Penocchio, B. M. W. Roberts, *Chem* 2023, 9, 2902–2917; d) J. M. Gallagher, B. M. W. Roberts, S. Borsley, D. A. Leigh, *Chem* 2024, 10, 1–12.
- [11] a) A. P. Davis, D. N. Sheppard, B. D. Smith, *Chem. Soc. Rev.* 2007, 36, 348–357; b) S. Matile, A. Vargas Jentzsch, A. Fin, J. Montenegro, *Chem. Soc. Rev.* 2011, 40, 2453–2474; c) N. Sakai, S. Matile, *Langmuir* 2013, 29, 9031–9040; d) S. J. Webb, *Acc. Chem. Res.* 2013, 46, 2878–2887.
- [12] M. Schliwa, G. Woehlke, *Nature* 2003, 422, 759–765.
- [13] a) G. Steinberg-Yfrach, P. A. Liddell, S.-C. Hung, A. L. Moore, D. Gust, T. A. Moore, *Nature* 1997, 385, 239–241; b) G. Steinberg-Yfrach, J.-L. Rigaud, E. N. Durantini, A. L. Moore, D. Gust, T. A. Moore, *Nature* 1998, 392, 479–482; c) L. M. Bennett, H. M. Vanegas Farfano, F. Bogani, A. Primak, P. A. Liddell, L. Otero, L. Sereno, J. J. Silber, A. L. Moore, T. A. Moore, D. Gust, *Nature* 2002, 420, 398–401; d) X. Xie, G. A. Crespo, G. Mistlberger, E. Bakker, *Nat. Chem.* 2014, 6, 202–207; e) E. N. W. Howe, P. A. Gale, *J. Am. Chem. Soc.* 2019, 141, 10654–10660; f) X. Wu, J. R. Small, A. Cataldo, A. M. Withecombe, P. Turner, P. A. Gale, *Angew. Chem. Int. Ed.* 2019, 58, 15142–15147; *Angew. Chem.* 2019, 131, 15286–15291.
- [14] a) M. A. Watson, S. L. Cockcroft, *Chem. Soc. Rev.* 2016, 45, 6118–6129; b) M. J. Langton, *Nat. Rev. Chem.* 2021, 5, 46–61; c) L. E. Bickerton, T. G. Johnson, A. Kerckhoffs, M. J. Langton *Chem. Sci.* 2021, 12, 11252–11274; d) T. G. Johnson, M. J. Langton, *J. Am. Chem. Soc.* 2023, 145, 27167–27184.
- [15] a) V. Balzani, A. Credi, F. M. Raymo, J. F. Stoddart, *Angew. Chem. Int. Ed.* 2000, 39, 3348–3391; b) J. W. Canary, *Chem. Soc. Rev.* 2009, 38, 747–756; c) A. Bianchi, E. Delgado-Pinar, E. García-España, C. Giorgi, F. Pina, *Coord. Chem. Rev.* 2014, 260, 156–215; d) V. Blanco, D. A. Leigh, V. Marcos, *Chem. Soc. Rev.* 2015, 44, 5341–5370; e) D. Sluysmans, J. F. Stoddart, *Trends Chem.* 2019, 1, 185–197.
- [16] a) N. Koumura, R. W. J. Zijlstra, R. A. van Delden, N. Harada, B. L. Feringa, *Nature* 1999, 401, 152–155; b) N. Koumura, E. M. Geertsema, M. B. van Gelder, A. Meetsma, B. L. Feringa, *J. Am. Chem. Soc.* 2002, 124, 5037–5051; c) D. A. Leigh, J. K. Y. Wong, F. Dehez, F. Zerbetto, *Nature* 2003, 424, 174–179; d) S. P. Fletcher, F. Dumur, M. M. Pollard, B. L. Feringa, *Science* 2005, 310, 80–82; e) M. von Delius, E. M. Geertsema, D. A. Leigh, *Nat. Chem.* 2010, 2, 96–101; f) G. Ragazzon, M. Baroncini, S. Silvi, M. Venturi, A. Credi, *Nat. Nanotechnol.* 2015, 10, 70–75; g) C.

- Cheng, P. R. McGonigal, S. T. Schneebeli, H. Li, N. A. Vermeulen, C. Ke, J. F. Stoddart, *Nat. Nanotechnol.* **2015**, *10*, 547–553; h) B. S. L. Collins, J. C. M. Kistemaker, E. Otten, B. L. Feringa, *Nat. Chem.* **2016**, *8*, 860–866; i) S. Erbas-Cakmak, S. D. P. Fielden, U. Karaca, D. A. Leigh, C. T. McTernan, D. J. Tetlow, M. R. Wilson, *Science* **2017**, *358*, 340–343; j) L. Zhang, Y. Qiu, W.-G. Liu, H. Chen, D. Shen, B. Song, K. Cai, H. Wu, Y. Jiao, Y. Feng, J. S. W. Seale, C. Pezzato, J. Tian, Y. Tan, X.-Y. Chen, Q.-H. Guo, C. L. Stern, D. Philp, R. D. Astumian, W. A. Goddard III, J. F. Stoddart, *Nature* **2023**, *613*, 280–286.
- [17] a) M. R. Wilson, J. Solà, A. Carlone, S. M. Goldup, N. Lebrasseur, D. A. Leigh, *Nature* **2016**, *534*, 235–240; b) S. Amano, S. D. P. Fielden, D. A. Leigh, *Nature* **2021**, *596*, 529–534; c) S. Borsley, E. Kreidt, D. A. Leigh, B. M. W. Roberts, *Nature* **2022**, *604*, 80–85.
- [18] S. Borsley, D. A. Leigh, B. M. W. Roberts, *Nat. Chem.* **2022**, *14*, 728–738.
- [19] a) L. S. Kariyawasam, C. S. Hartley, *J. Am. Chem. Soc.* **2017**, *139*, 11949–11955; b) M. Tena-Solsona, B. Rieß, R. K. Grötsch, F. C. Löhner, C. Wanzke, B. Käs Dorf, A. R. Bausch, P. Müller-Buschbaum, O. Lieleg, J. Boekhoven, *Nat. Commun.* **2017**, *8*, 15895; c) B. Rieß, R. K. Grötsch, J. Boekhoven, *Chem* **2020**, *6*, 552–578; d) P. Schwarz, M. Tena-Solsona, K. Dai, J. Boekhoven, *Chem. Commun.* **2022**, *58*, 1284–1297.
- [20] R. D. Astumian, S. Mukherjee, A. Warshel, *ChemPhysChem* **2016**, *17*, 1719–1741.
- [21] a) C. J. E. Haynes, J. Zhu, C. Chimere, S. Hernández-Ainsa, I. A. Riddell, T. K. Ronson, U. F. Keyser, J. R. Nitschke, *Angew. Chem. Int. Ed.* **2017**, *56*, 15388–15392; b) Q. Xiao, W. W. Haoyang, T. Lin, Z. T. Li, D. W. Zhang, J. L. Hou, *Chem. Commun.* **2021**, *57*, 863–866; c) T. Yan, S. Liu, C. Li, J. Xu, S. Yu, T. Wang, H. Sun, J. Liu, *Angew. Chem. Int. Ed.* **2022**, *61*, e202210214; d) P. V. Jog, M. S. Gin, *Org. Lett.* **2008**, *10*, 3693–3696; e) A. Koçer, M. Walko, W. Meijberg, B. L. Feringa, *Science* **2005**, *309*, 755–758; f) Y. Zhou, Y. Chen, P. P. Zhu, W. Si, J. L. Hou, Y. Liu, *Chem. Commun.* **2017**, *53*, 3681–3684; g) R. Y. Yang, C. Y. Bao, Q. N. Lin, L. Y. Zhu, *Chin. Chem. Lett.* **2015**, *26*, 851–856; h) T. Liu, C. Bao, H. Wang, Y. Lin, H. Jia, L. Zhu, *Chem. Commun.* **2013**, *49*, 10311–10313; i) P. Talukdar, G. Bollot, J. Mareda, N. Sakai, S. Matile, *Chem. Eur. J.* **2005**, *11*, 6525–6532; j) P. Talukdar, G. Bollot, J. Mareda, N. Sakai, S. Matile, *J. Am. Chem. Soc.* **2005**, *127*, 6528–6529; k) S. Bhosale, A. L. Sisson, P. Talukdar, A. Fürstenberg, N. Banerji, E. Vauthey, D. Bollot, J. Mareda, C. Röger, F. Würthner, N. Sakai, S. Matile, *Science* **2006**, *313*, 84–86; l) A. D. Peters, S. Borsley, F. della Sala, D. F. Cairns-Gibson, M. Leonidou, J. Clayden, G. F. S. Whitehead, I. J. Vitorica-Yrezabal, E. Takano, J. Burthem, S. L. Cockroft, S. J. Webb, *Chem. Sci.* **2020**, *11*, 7023–7030.
- [22] a) S. Shinkai, T. Ogawa, T. Nakaji, O. Manabe, *J. Chem. Soc., Chem. Commun.* **1980**, 375b–377; b) S. Shinkai, T. Nakaji, T. Ogawa, K. Shigematsu, O. Manabe, *J. Am. Chem. Soc.* **1981**, *103*, 111–115; c) S. Shinkai, K. Shigematsu, M. Sato, O. Manabe, *J. Chem. Soc., Perkin Trans. 1* **1982**, 2735–2739; d) T. Jin, *Chem. Commun.* **2000**, 1379–1380; e) T. Jin, *Mater. Lett.* **2007**, *61*, 805–808; f) Y. R. Choi, G. C. Kim, H. G. Jeon, J. Park, W. Namkung, K. S. Jeong, *Chem. Commun.* **2014**, *50*, 15305–15308; g) M. Ahmad, S. Chattopadhyay, D. Mondal, T. Vijayakanth, P. Talukdar, *Org. Lett.* **2021**, *23*, 7319–7324; h) A. Kerckhoffs, M. J. Langton, *Chem. Sci.* **2020**, *11*, 6325–6331; i) A. Kerckhoffs, Z. Bo, S. E. Penty, F. Duarte, M. J. Langton, *Org. Biomol. Chem.* **2021**, *19*, 9058–9067; j) S. J. Wezenberg, L. J. Chen, J. E. Bos, B. L. Feringa, E. N. W. Howe, X. Wu, M. A. Siegler, P. A. Gale, *J. Am. Chem. Soc.* **2022**, *144*, 331–338; k) D. Villarón, J. E. Bos, F. Kohl, S. Mommer, J. de Jong, S. J. Wezenberg, *J. Org. Chem.* **2023**, *88*, 11328–11334; l) J. N. Martins, B. Raimundo, A. Rioboo, Y. Folgar-Cameán, J. Montenegro, N. Basílio, *J. Am. Chem. Soc.* **2023**, *145*, 13126–13133.
- [23] A. K. Dambeniaks, P. H. Q. Vua, T. M. Fyles, *Chem. Sci.* **2014**, *5*, 3396–3403.
- [24] T. Longin, M. L. Goyette, C. A. Koval, *Chem. Innov.* **2001**, *31*, 23–30.
- [25] a) T. Muraoka, D. Noguchi, R. S. Kasai, K. Sato, R. Sasaki, K. V. Tabata, T. Ekimoto, M. Ikeguchi, K. Kamagata, N. Hoshino, H. Noji, T. Akutagawa, K. Ichimura, K. Kinbara, *Nat. Commun.* **2020**, *11*, 2924; b) R. Sasaki, K. Sato, K. V. Tabata, H. Noji, K. Kinbara, *J. Am. Chem. Soc.* **2021**, *143*, 1348–1355.
- [26] a) C. F. Higgins, *Res. Microbiol.* **2001**, *152*, 205–210; b) C. F. Higgins, K. J. Linton, *Nat. Struct. Mol. Biol.* **2004**, *11*, 918–926; c) K. P. Locher, *Nat. Struct. Mol. Biol.* **2016**, *23*, 487–493; d) C. Thomas, R. Tampé, *Annu. Rev. Biochem.* **2020**, *89*, 605–636.
- [27] a) U. Hopfer, *J. Theor. Biol.* **2002**, *214*, 539–547; b) S. Flatt, D. M. Busiello, S. Zamuner, P. De Los Rios, *Commun. Phys.* **2023**, *6*, 205.
- [28] a) S. Amano, S. Borsley, D. A. Leigh, Z. Sun, *Nat. Nanotechnol.* **2021**, *16*, 1057–1067; b) T. Sangchai, S. Al Shehimi, E. Penocchio, G. Ragazzon, *Angew. Chem. Int. Ed.* **2023**, *62*, e202309501; c) S. Borsley, J. M. Gallagher, D. A. Leigh, B. M. W. Roberts, *Nat. Rev. Chem.* **2023**, in press.
- [29] a) D. Gust, T. A. Moore, A. L. Moore, *Acc. Chem. Res.* **2009**, *42*, 1890–1898; b) D. G. Nocera, *Acc. Chem. Res.* **2012**, *45*, 767–776; c) Z. Hameiri, *Prog. Photovolt.* **2018**, *26*, 234–238; d) T. Keijer, T. Bouwens, J. Hessels, J. N. H. Reek, *Chem. Sci.* **2021**, *12*, 50–70.
- [30] a) I. C. Pintre, S. J. Webb, *Adv. Phys. Org. Chem.* **2013**, *47*, 129–183; b) X. Wu, P. Wang, W. Lewis, Y.-B. Jiang, P. A. Gale, *Nat. Commun.* **2022**, *13*, 4623.
- [31] a) S. M. Morrow, I. Colomer, S. P. Fletcher, *Nat. Commun.* **2019**, *10*, 1011; b) D. Babu, R. J. H. Scanes, R. Plamont, A. Ryabchun, F. Lancia, T. Kudernac, S. P. Fletcher, N. Katsonis, *Nat. Commun.* **2021**, *12*, 2959; c) M. G. Howlett, A. H. J. Engwerda, R. J. H. Scanes, S. P. Fletcher, *Nat. Chem.* **2022**, *14*, 805–810; d) A. M. Bergmann, J. Bauermann, G. Bartolucci, C. Donau, M. Stasi, A.-L. Holtmannspötter, F. Jülicher, C. A. Weber, J. Boekhoven, *Nat. Commun.* **2023**, *14*, 6552.

Manuscript received: January 11, 2024

Accepted manuscript online: February 9, 2024

Version of record online: March 4, 2024